TECHNICAL BULLETIN NO. 3

GEOPIER® UPLIFT RESISTANCE

This Technical Bulletin discusses the behavior of Geopier Rammed Aggregate Pier® elements when subject to uplift (tensile) loads. Tensile loads are often applied to foundation systems when the supported structures are subject to wind or seismic loads. Uplift anchors are incorporated into Geopier elements to resist these tensile loads. The anchors consist of a steel plate installed at the bottom of the piers and threaded bars connected to and extending from the embedded plate to the overlying footing. This Technical Bulletin describes structure uplift loading demands, Geopier uplift anchor construction, pull-out resistance of individual elements and groups of elements, and load-deflection response.

1. BACKGROUND: STRUCTURE UPLIFT DEMANDS

Buildings are subject to applied lateral loads during windstorms and seismic events. The applied lateral loads form an overturning moment that must be resisted by compression and tensile forces at the building foundation (Figure 1). If the applied foundation tensile force is greater than the static downward force, the footing may lift off the ground and lead to structural instability. Geopier uplift elements are designed to resist these tensile loads.

The appropriate factor of safety used in the design of uplift elements depends on a variety of factors including: 1) whether or not a load test is performed at the site, 2) the rate of anticipated loading applied to the structure, and 3) the directionality of loading.

Based on the Geopier element uplift test, which is usually performed at locations that exhibit the weakest soil conditions, a factor of safety of 2.0 is usually considered appropriate for the resistance of sustained uplift loads. If the elements are used to resist seismic loadings, lower factors of safety may be used because the dynamic resistance of the anchors is greater than the static (tested) resistance of the anchors and because loading directions reverse over short time periods thereby minimizing the possibility of sustained uplift.

GEOPIER®
Tensar

Figure 1.
Building Subjected to Lateral Loads

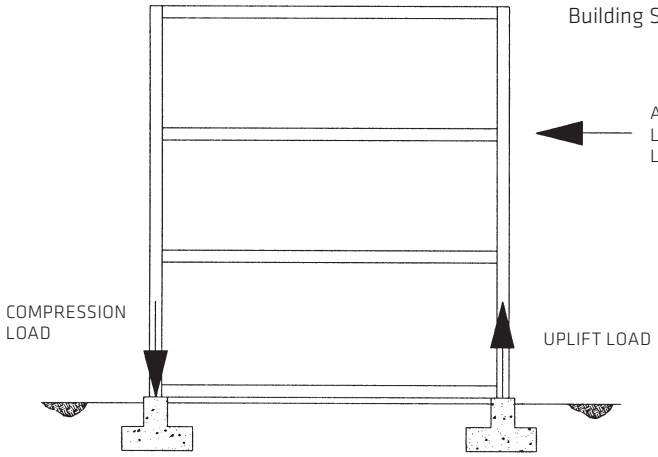

2. CONSTRUCTION

A constructed Geopier uplift element with matrix soil stress response is shown on Figure 2. Geopier element shafts are excavated to the required drill depth and the bottom bulb is constructed with open-graded stone. An uplift harness is then lowered into the hole to the top of the densified bottom bulb. The anchor consists of a round or rectangular steel plate with tie rods connected at the outer edge of the plate. Typical assemblies incorporate either two or four uplift rods. After the uplift harness is installed, the remainder of the Geopier element is constructed by ramming aggregate in thin lifts with a beveled tamper. The uplift rods must be spaced sufficiently far apart so that the tamper can fit between the rods as the pier is constructed. The uplift rods are connected to the overlying footing via standard hooks and other structural connections.

Figure 2.
Geopier Uplift Element

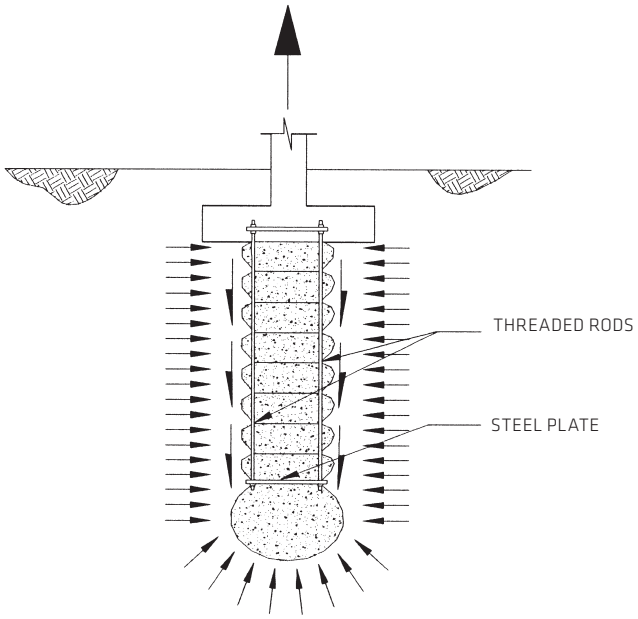

3. BACKGROUND

A significant amount of research effort has been focused on the orientation of the failure surfaces that develop during pullout of conventional embedded anchors (Charlie et al, 1985; Kulhawy et al, 1979; Meyerhof & Adams, 1968; Vesic, 1975; Ghaly et al, 1991). Field observations for conventional embedded anchors indicate that the rupture surface corresponds to either 1) an upright cylinder with a perimeter defined by the footprint of the embedded anchor or 2) a surface that, at the ground surface, is larger than the perimeter of the anchor. Kulhawy (1985) suggests that as upward forces are applied, shear stresses develop along inclined shearing planes (Figure 3) that satisfy Mohr-Coulomb failure criterion. With additional movement, vertical displacement shearing surfaces develop, resulting in continuing upward displacements. This shear pattern will propagate very close to the interface, essentially defining the perimeter of the uplift anchor.

When anchors with small aspect ratios are installed in relatively high strength soils, the inclined shearing surfaces may daylight at the ground surface. This failure mechanism results in a conical failure surface. The failure surface then is represented by a cylindrical surface at depth transitioning into a conical surface that daylights at some distances from the perimeter of the element. Although Kulhawy has developed solutions for the conical failure surface, solutions for a continuous cylindrical surface provide nearly the same uplift resistance.

Figure 3.
Shearing Stresses on Embedded Anchor (after Kulhawy, 1985)

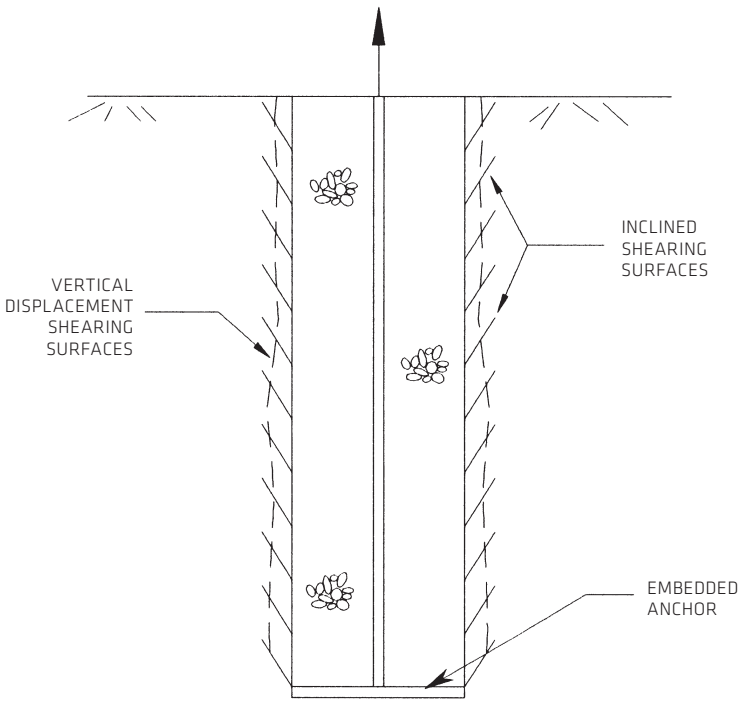

4. PULL-OUT RESISTANCE OF INDIVIDUAL UPLIFT ELEMENTS

Observations of Geopier elements that have been pulled completely out of the ground during Geopier uplift research efforts indicate that the critical shearing surface is cylindrical and occurs at the perimeter of the installed element (Figure 2). Prior to complete pullout failure, radial and circumferential cracks are often observed at the ground surface. These cracking patterns are consistent with the near surface inverted conical failure surfaces described in the literature for embedded anchors loaded in tension (Kulhawy, 1985). The approach used to compute the pull-out resistance of individual Geopier elements is presented in Figure 4. When Geopier elements are subjected to extreme uplift loads, a cylindrical failure surface forms around the elements. The ultimate pull-out resistance (Q_{ult}) is computed as the sum of the weight of the Geopier element (W) and the side resistance. The ultimate side resistance is computed as the product of the unit pullout resistance (f_s) and the area of the sheared cylinder (A_s):

$$Q_{ult} = W + f_s A_s = W + f_s \pi d H_s \qquad \text{Eq. 1.}$$

where W is the buoyant weight of the Geopier elment, d is the effective diameter of the Geopier element, H_s is the shaft length of the element (Figure 4). The effective Geopier diameter is generally greater than the drilled diameter as a result of ramming the Geopier aggregate.

Figure 4.
Individual Geopier Pullout Resistance

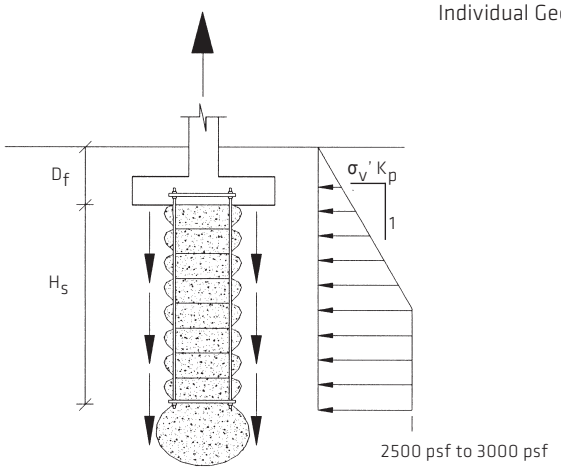

4.1 COHESIONLESS SOILS

For Geopier elements installed in cohesionless soils, the rate of drainage is typically faster than the net increases in uplift during cumulative cycles of loading. The uplift loading resistance of individual Geopier elements is therefore computed using drained geotechnical analysis procedures. The unit friction (f_s) is computed as the sum of the drained cohesion intercept (c) and the product of the lateral pressure in the soil surrounding the Geopier elements (σ_h') and the tangent of the angle of internal friction of the matrix soils (φ'_m):

$$f_s = c + \sigma_h' \tan(\varphi'_m) \qquad \text{Eq. 2.}$$

The drained cohesion intercept (c) is often considered to be zero for clean sands and gravels.

The ramming action inherent in Geopier construction increases the lateral earth pressure in the matrix soils surrounding the Geopier elements. The increase in lateral stress is dependent upon soil type, drainage, overconsolidation ratio, and confinement offered by adjacent Geopier elements. Post-construction lateral earth pressure is typically computed as the product of the geostatic vertical stress in the matrix soils (σ_v') and the Rankine passive earth pressure coefficient (K_p):

$$\sigma_h' = \sigma_v' K_p \ , \qquad \text{Eq. 3.}$$

where:

$$K_p = \tan^2 (45+\varphi'_m /2). \qquad \text{Eq. 4.}$$

As shown in Figure 4, the applied lateral earth pressure is limited by a value ranging between approximately 2,500 psf (120 kPa) to 3,000 psf (144 kPa) to conservatively account for the maximum energy that is typically imparted by the Geopier hammer to the surrounding soils (Handy 2001).

4.2 COHESIVE SOILS

When Geopier elements are installed in cohesive soils, the rate of uplift loading may or may not be less than the rate of drainage. Therefore, the unit friction (f_s) is computed as the smaller of 1) the undrained shear strength (s_u) of the matrix soils and 2) the drained unit friction of the matrix soils using Equation 2, above. The ultimate uplift capacity (Qult) thus becomes the smaller of:

$$Q_{ult} = (c + \sigma_h' \tan (\varphi'_m)) \pi d H_s + W, \qquad \text{Eq. 5.}$$

and

$$Q_{ult} = s_u \pi d H_s + W \qquad \text{Eq. 6.}$$

4.3 DESIGN OF UPLIFT RODS

High strength, threaded steel rods, such as those produced by Dywidag or Williams, are typically used within the uplift harnesses. The allowable tension load for each rod (Q_{rod}) is computed as the product of the allowable tensile stress of the steel (F_{all}) and the bar cross-sectional area (A_{rod}):

$$Q_{rod} = F_{all} \cdot A_{rod} = F_{all} \cdot \pi \cdot d^2_{rod} /4 \qquad \text{Eq. 7.}$$

where d_{rod} is the uplift rod diameter. Most codes suggest the allowable tensile stress may not exceed 60% of the steel yield strength:

$$F_{all} = 0.60 F_y \qquad \text{Eq. 8.}$$

The design of the uplift bars should consider corrosion. Bars may be galvanized, epoxy-coated or designed with sufficient sacrificial steel to account for corrosion over the design life of the structure.

4.4 DESIGN OF UPLIFT RODS

The design methods described above and selected design parameter values should be verified with an uplift load test if the elements are used to resist significant tension loads.

5. GROUP EFFECTS

The uplift capacity of groups of closely-spaced Geopier elements is computed as the smaller of: 1) the uplift capacity of a single element multiplied by the total number of elements, and 2) the uplift capacity of a soil block subject to tension (Figure 5). For Geopier elements installed in cohesionless soils, the volume of the block is defined by the footprint of the overlying footing and sloping sidewalls as shown in Figure 5a. The inclination angle of the sidewalls of the block (β) depends on the matrix soil angle of internal friction and on the lateral earth pressure induced by the construction of the Geopier element. Values ranging from 15 degrees to 20 degrees are often used for β in the design calculations. The uplift resistance is computed as the buoyant weight of the soil contained within the block:

$$Q_{block} = W_{block}. \qquad \text{Eq. 9.}$$

For Geopier elements installed in cohesive soils, the volume of the block is defined by the area of the footing footprint and vertical sidewalls as shown in Figure 5b. The uplift resistance is computed by summing the total weight of the soil within the block and the undrained shearing resistance along the edges of the block:

$$Q_{block} = W_{block} + s_u\,(2B' + 2L')\,H_s, \qquad \text{Eq. 10.}$$

where B' and L' are the dimensions of the footprint of the soil block.

Figure 5.
Group Uplift Capacity for Closely-Spaced Geopier Elements

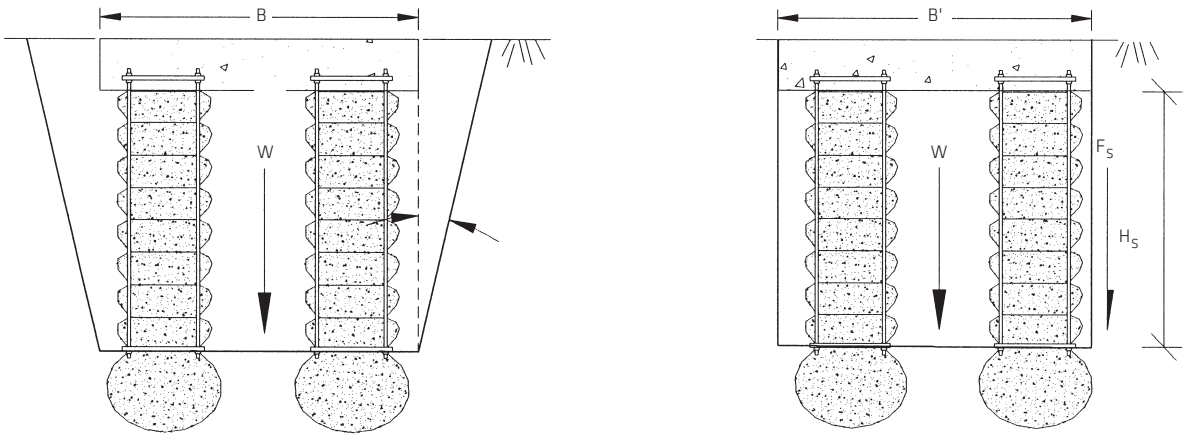

a. COHESIONLESS SOILS

b. COHESIVE SOILS

6. UPLIFT LOAD TESTS

Uplift load tests are often performed on test Geopier elements. The tests are typically located at an area of the site containing the weakest identified soil conditions. A typical test setup is shown in Figure 6. The uplift rods are connected to a cross-member on top of the test reaction beam. During testing, a jack extends the distance between the cross-member and the reaction beam thus pulling on the uplift rods and applying tensile loads to the Geopier element. Load testing is typically performed in general agreement with ASTM D-1144 specifications and from one to four days after test pier installation to allow time for the dissipation of matrix soil excess pore water pressures. Uplift load tests are used to verify the design uplift capacity.

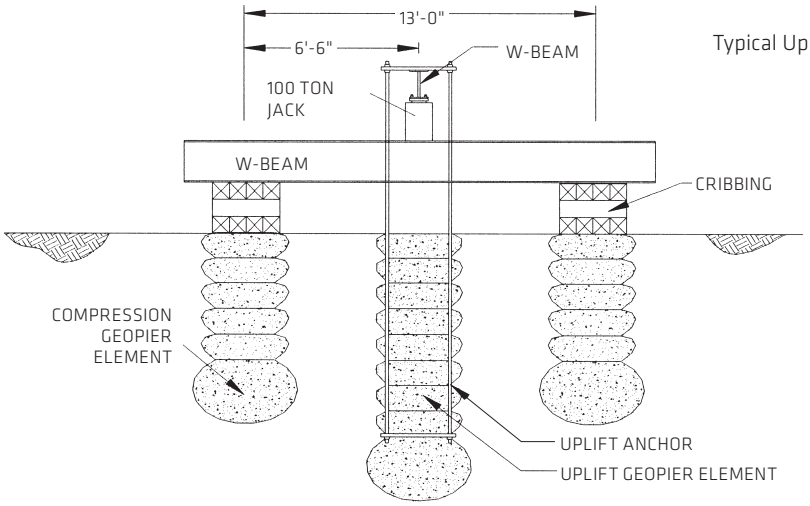

Figure 6.
Typical Uplift Load Test Setup

7. UPLIFT LOAD-DEFLECTION RESPONSE

7.1 INTERPRETATION OF UPLIFT LOAD TEST RESULTS

Figure 7 illustrates a characteristic plot of uplift test results. The results typically consist of three straight-line segments. The first segment corresponds to the seating of the uplift plate and rearrangement of aggregate particles within the lower part of the Geopier element. The slope of this line, designated m_1, is generally small. The second segment represents upward deflection of the bottom plate caused by bulging of the lower portion of the pier and movement along the cylindrical sides of the element. This segment trends at a slope, m_2, until shearing failure occurs. The third segment is vertical or near-vertical and represents conditions at which excessive deflections occur with no or minimal additional application of loads. The ultimate uplift capacity is interpreted to occur at the intersection of the second and third line segments.

Figure 7.
Uplift Test Results

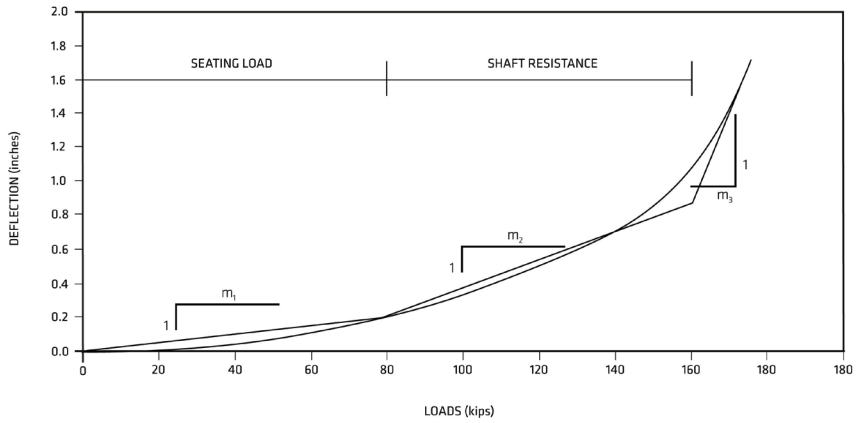

7.2 TYPICAL DEFLECTIONS

Uplift deflection control is often important to maintain structural performance. Table 1 presents a summary of deflections measured for 30-inch diameter elements during uplift load tests conducted within gravel, sand, and silt/clay deposits. The deflection values include the elastic elongation of the uplift rods. Table 1 may be used to aid in predicting upward deflections for various levels of applied uplift loads. In general, uplift deflections increase with decreasing matrix soil grain size.

Table 1.
Summary of Uplift Load Test Deflection

SOIL	LOAD [AVERAGE OF VALUES] (KIPS)	SEATING DEFLECTION [AVERAGE OF VALUES] (IN/KIP)	SKIN FRICTION DEFLECTION [AVERAGE OF VALUES] (IN/KIP)
GRAVEL	40-90 [60]	0.005 - 0.006 [0.005]	0.004 - 0.009 [0.006]
SAND	30-55 [43]	0.004 - 0.007 [0.005]	0.004 - 0.007 [0.013]
SILT AND CLAY	20-60 [41]	0.004 - 0.009 [0.006]	0.009 - 0.033 [0.015]

If the steel uplift plates are installed in soft clay or silt that exhibit the tendency to bulge outward during uplift load applications (Figure 8), the deflections of uplift elements may be greater than those presented in Table 1, above. Methods used to estimate bulging potential are provided in Geopier Foundation Company's Technical Bulletin No. 2: Bearing Capacity. The ultimate uplift capacity may be estimated by the product of the limiting radial stress ($\sigma'_{r,lim}$), the Rankine passive earth pressure coefficient of the Geopier aggregate material, and the cross-sectional area of the element:

$$Q_{ult} = \sigma'_{r,lim} \tan^2(45 + \varphi'_g/2)\, \pi\, d^2/4. \qquad \text{Eq. 11.}$$

The limiting radial stress is computed as:

$$\sigma'_{r,lim} = 2\, \sigma'_v + 5.2\, s_u. \qquad \text{Eq. 12.}$$

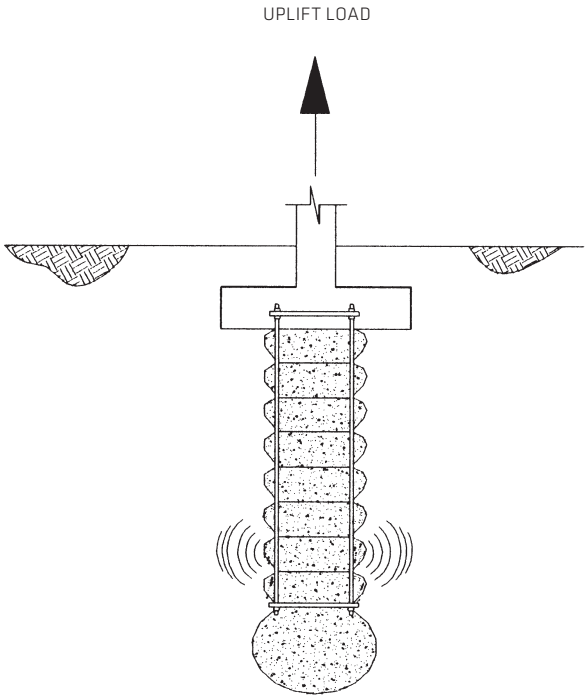

Figure 8.
Outward Bulging Element

8. SUMMARY

Geopier uplift elements resist applied uplift loads by developing resistance between the perimeter of the elements and the surrounding matrix soils. The elements are particularly efficient because of the increase in matrix soil lateral stress that occurs during construction. The elements are used to provide stability to shallow spread footings that are subjected to tensile loads.

AUTHORS

Kord J. Wissmann, Ph.D., P.E.

Brendan T. FitzPatrick, P.E.

REFERENCES

Caskey, J.M. (2001). "Uplift Capacity of Rammed Aggregate Pier Soil Reinforcing Elements." MS thesis in preparation. University of Memphis.

Charlie, W.A., Turner, J.P., and Kulhawy, F.H. (1985). "Review of Repeated Axial Load Tests on Deep Foundations", Drilled Piers and Caissons II. Ed. By C.N. Baker, ASCE, New York, May 1985, pp. 129-150.

Ghaly, A., Hanna, A., Hanna, M. (1991). "Uplift Behavior of Screw Anchors in Sand. I: Dry Sand." Journal of Geotechnical Engineering, Vol. 117, No. 5, May 1991, pp. 773-93.

Handy, R L. (2001). Personal communication. March 1, 2001. Hsu, C. L. (2000). "Uplift Capacity of Geopier Foundations." MS thesis. University of Utah.

Kulhawy, F.H. (1985). "Uplift behavior of shallow soil anchors – an overview." Uplift Behavior of Anchor Foundations in Soil, Special Publication. Clemence (editor), American Society of Civil Engineers, 1-25.

Kulhawy, F.H., Kozera, D.W., and Withiam, J.L. (1979). "Uplift Testing of Model Drilled Shafts in Sand." Journal of Geotechnical Engineering Division. ASCE, Vol. 105, GT1, Jan 1979, pp. 31-47.

Lawton, E. C. (2000). "Performance of Geopier Foundations During Simulated Seismic Tests at South Temple Bridge on Interstate 15, Salt Lake City, Utah." Final Report, No. UUCVEEN 00-03, University of Utah, Salt Lake City, Utah.

Lawton E. C. and N. S. Fox. (1994). "Settlement of structures supported on marginal or inadequate soils stiffened with short aggregate piers." Vertical and Horizontal Deformations of Foundations and Embankments, A.T. Yeung and G.Y. Fello (Editors), American Society of Civil Engineers, 2, 962-74.

Lawton, E.C., Fox, N. S., and R. L. Handy. (1994). "Control of settlement and uplift of structures using short aggregate piers." In-situ Deep Soil Improvement, K.M. Rollins (Editor), American Society of Civil Engineers, 121-132.

Meyerhof, G.G. and Adams, J.I. (1968). "The Ultimate Uplift Capacity of Foundations." Canadian Geotechnical Journal. Vol. 5, No. 4, Nov 1968, pp. 225-244.

NAVFAC. (1982). Foundations and Earth Structures – Design Manual 7.2. Department of the Navy. 7.2-205 – 207.Vesic, A.S. (1975). "Bearing Capacity of Shallow Foundations." Chap. 3 in Foundation Engineering Handbook, Ed. By H. Winterkorn and H.Y. Fang, Van Nostrand Reinhold Co., New York, 1975, pp. 121-147.

ACKNOWLEDGEMENTS

Uplift load test data summarized herein have been provided by Geopier Foundation Company, Inc, GFC West, Inc., GFC Northwest, Inc., Geopier Foundation Company of Northern California, Peterson Contractors, Inc., GeoStructures, Inc., GeoConstructors, Inc., and the University of Utah. The authors wish to thank Professor Richard Handy, Professor David White, Professor Evert Lawton, Mr. John Martin, Mr. Michael Cowell, and Mr. Tom Farrell for their careful review and helpful comments.

GEOPIER IS GROUND IMPROVEMENT®

Work with engineers worldwide to solve your ground improvement challenges.
For more information call 800-371-7470, email info@geopier.com, or visit geopier.com.

130 Harbour Place Drive, Suite 280, Davidson, NC 28036
800.371.7470 | info@geopier.com | marketing@geopier.com
www.geopier.com

GEOPIER®
Tensar

GEOPIER_TB_3_01.16